CNS Spectrums

www.cambridge.org/cns

Exploring resting-state network dysconnectivity in schizophrenia with single-subject ICA

Margherita Biondi[1], Marco Marino[2,3], Dante Mantini[3] and Chiara Spironelli[1,2]

[1]Padova Neuroscience Center, University of Padova, Padova, Italy; [2]Department of General Psychology, University of Padova, Italy and [3]Movement Control and Neuroplasticity Research Group, Katholieke Universiteit Leuven, Belgium

Original Research

Cite this article: Biondi M, Marino M, Mantini D, and Spironelli C (2026). Exploring resting-state network dysconnectivity in schizophrenia with single-subject ICA. *CNS Spectrums*, **31**(1), e15, 1–12.
https://doi.org/10.1017/S1092852926100959

Received: 22 January 2026
Accepted: 09 May 2026

Key words:
Independent component analysis (ICA); functional magnetic resonance imaging (fMRI); single-subject analysis; default mode network (DMN); resting-state network (RSN); schizophrenia (SZ)

Corresponding author:
Chiara Spironelli;
Email: chiara.spironelli@unipd.it

Abstract

Objective. Resting-state networks (RSNs) consist of coherent spontaneous activity patterns that support a wide range of sensorimotor and higher-order cognitive functions. In schizophrenia (SZ), RSN alterations reflect disruptions in the brain's functional architecture. Given the heterogeneity of SZ, accurate spatial mapping of RSNs at the individual level is crucial for characterizing altered brain connectivity in a more personalized manner. To achieve this, we used single-subject independent component analysis (ICA) to extract RSNs at the individual level, preserving unique functional patterns and accounting for variability among SZ patients.

Methods. We analyzed a resting-state functional magnetic resonance imaging dataset from 74 SZ patients and 74 matched healthy controls (HCs) obtained from the publicly available COINS database. Using single-subject ICA, we extracted 14 distinct RSNs associated with sensory, motor, and higher-order cognitive functions. Voxel-wise statistical comparisons were performed to identify spatial differences between the groups.

Results. The SZ group exhibited widespread RSN alterations in regions associated with visual, motor, and cognitive processing. Significant spatial differences were observed within each network, with the most extensive changes occurring in the somatomotor network and three cognitive networks: the cingulo-insular, medial prefrontal, and left frontoparietal networks. Within the default mode network, differences between SZ patients and HC were observed exclusively in visual areas.

Conclusions. Single-subject ICA provides a valuable approach for investigating RSN alterations in SZ and enables a detailed, individualized characterization of functional connectivity disruptions. The extensive connectivity alterations in visual, motor, and cognitive networks highlight the complex interplay among these systems in SZ.

Introduction

Over the past two decades, studies have demonstrated that spontaneous brain activity organizes into specific patterns that reflect the functional architecture of the brain.[1] These functional patterns, known as resting-state networks (RSNs), are typically measured using functional magnetic resonance imaging (fMRI), through spontaneous fluctuations in the blood-oxygen-level-dependent signal observed during rest, that is, in the absence of task engagement.[2]

In clinical neuroscience, the ability to accurately characterize brain functional connectivity patterns is of crucial importance. The detailed mapping of RSNs is particularly valuable for understanding complex disorders like schizophrenia (SZ), where dysconnectivity has been identified as a core mechanism.[3–7] Starting with the seminal works of Friston and Andreasen,[4,5] SZ has increasingly been conceptualized as a disorder of abnormal anatomical and functional connectivity, affecting key networks involved in perceptual, cognitive, and emotional processing.[6,7] Resting-state fMRI (rs-fMRI) has proven to be a powerful tool for identifying baseline disruptions in large-scale brain networks without the confounding effects of task-based constraints.[8] Moreover, the absence of tasks during scanning provides a key advantage for clinical applications, as it facilitates the use of rs-fMRI in patients with limited cooperation or difficulty performing tasks.[9]

Among the pioneering research on the role of spontaneous brain activity,[10–12] the study by Mantini et al. was pivotal in revealing how RSNs support brain function.[13] This study demonstrated that RSNs are characterized not only by specific anatomical correlates but also by unique electrophysiological signatures, providing the first evidence of a link between fast neural processes and RSNs. This finding offered new insights into their role in sensory, motor, and cognitive functions, independent of task-evoked activity.[13] Since then, the resting-state approach has been increasingly employed to investigate how RSNs contribute to brain function in healthy individuals and how they are altered in pathological conditions.[14,15]

The default mode network (DMN) is among the most extensively studied RSNs. This network includes brain regions primarily involved in internally focused cognitive processes, such as self-

© The Author(s), 2026. Published by Cambridge University Press. This is an Open Access article, distributed under the terms of the Creative Commons Attribution-NonCommercial licence (http://creativecommons.org/licenses/by-nc/4.0), which permits non-commercial re-use, distribution, and reproduction in any medium, provided the original article is properly cited. The written permission of Cambridge University Press or the rights holder(s) must be obtained prior to any commercial use.

referential thinking, autobiographical memory retrieval, and mind-wandering.[16] The DMN plays a central role in spontaneous brain activity, emerging during restful, task-free states, and diminishing during attention-demanding tasks.[17] Alterations in the DMN have been widely implicated in various neurological disorders, including Alzheimer's disease, Parkinson's disease, and epilepsy,[18] as well as psychiatric conditions such as SZ, mood disorders, and anxiety disorders.[19]

Beyond the DMN, several other RSNs support a wide range of sensorimotor and higher-order cognitive functions. Mantini et al. identified 14 RSNs using independent component analysis (ICA), a data-driven statistical method that extracts maximally independent patterns of synchronized fMRI activity.[20,21] These RSNs encompass distinct functional domains, including sensory-motor functions, language, attention, and associative cognitive processes like salience processing, self-referential thinking, and emotional regulation.[20]

For example, the visual network (VN) is divided into the parafoveal and peripheral components, which together underlie visual sensory experiences and their integration into attention, memory, learning, and behavior.[22] The somatomotor network (SMN), comprising dorsal and ventral subdivisions, integrates sensory and motor inputs for movement programming and execution and supports complex cognitive functions such as spatial navigation.[23] The auditory network (AN) supports auditory functions, from the processing of acoustic stimuli to their higher-level integration.[24] The language network (LN) facilitates language production and comprehension, including phonological, lexical, semantic processing, and linguistic memory.[25] The dorsal attention network (DAN) and ventral attention network (VAN) interact to allocate attentional resources: the DAN is primarily involved in goal-directed, top-down attention, while the VAN is responsible for stimulus-driven, bottom-up attention.[26] Additionally, the left and right frontoparietal networks (lFPN and rFPN, respectively) are crucial for executive functions, such as working memory, inhibitory control, and planning.[27] The lateral and medial prefrontal networks (PFNs) are associated with executive control and self-referential thinking, respectively.[28,29] Finally, the cingulo-insular network (CIN) integrates cognition and emotion, monitoring interoceptive states and detecting salient stimuli.[30]

In the context of SZ, studies have primarily focused on alterations in the DMN, attention networks, and perceptual networks.[31,32] However, a fine-grained spatial comparison of RSNs between SZ patients and healthy controls (HCs) is still lacking.

To address this gap, we employed a single-subject ICA approach,[21] which allows for the extraction of RSNs at an individual level while preserving unique functional patterns and accounting for across-subject variability, a crucial aspect for heterogeneous conditions like SZ.[32] In this context, single-subject ICA preserves the uniqueness of each patient's neural characteristics, providing a potentially clinically relevant depiction of RSN alterations.[33]

Using this approach, we analyzed rs-fMRI data from SZ patients and HCs to explore differences in the spatial distribution of RSNs. Given the cognitive impairments associated with SZ,[34] we hypothesized that significant alterations compared to controls would be observed in networks related to cognitive functions.

Methods

Participants

The fMRI data used in this study were extracted from COINS (https://coins.trendscenter.org), an online, open-access database designed for research purposes that integrates data from multiple sources, including the Center for Biomedical Research Excellence (COBRE), MCIC (via the COINS database), the Functional Biomedical Informatics Research Network, XNAT Central, and the NUNDA and REDCap frameworks from Northwestern University. Access to these diverse data allows for large-scale studies with multi-site, multidimensional, and multimodal analyses. The present study focused on a sample of SZ patients and HC who met the following requirements: (1) availability of rs-fMRI images, (2) availability of T1 structural MRI (sMRI) images, and (3) availability of the complete Positive And Negative Syndrome Scale (PANSS) scores for the SZ sample.[35] Data from the COBRE project were used, collected from psychiatric patients at the UNM Psychiatric Center, the Raymond G. Murphy Veterans Affairs Medical Center, and other clinics in the Albuquerque metropolitan area (USA). The criteria for SZ patient inclusion were: (1) a diagnosis of SZ, confirmed by two psychiatrists using the DSM-IV Structured Clinical Interview for Axis I disorders (SCID)[36]; (2) clinical stability assessed both 3 months prior to and during the MRI sessions; (3) age between 18 and 65 years old.

Healthy participants were also recruited in Albuquerque, with the following exclusion criteria based on the Structured Clinical Interview (SCID)-Non-Patient edition: (1) diagnosis of past or current Axis I psychiatric disorder, (2) head trauma with loss of consciousness lasting more than 5 minutes, (3) recent substance abuse or antidepressant use within the past 5 months, and (4) having a first-degree relative with a psychotic disorder. All participants provided written informed consent in the original study. Data access was facilitated by the Collaborative Informatics and Neuroimaging Suite Data Exchange (COINS, http://coins.mrn.org/dx), and COBRE-funded data collection occurred at the Mind Research Network, subject to the licensing procedures (5P20RR021938/P20GM103472) from the National Institutes of Health to Dr. Vince Calhoun. All data were anonymized before access to protect participants' privacy. Structural and resting-state images were visually inspected to ensure the suitability of the sample.

MRI data acquisition

MRI data were acquired using a 3 T Siemens MR scanner (Trio, Siemens Healthcare, Erlangen, Germany). The acquisition protocol included sagittal-gradient echo scout images through the midline to obtain image slices that were axial, oblique, and parallel to the antero-posterior commissure line; in particular, oblique slices were used to minimize orbitofrontal susceptibility artifacts. rs-fMRI data were collected over 5 minutes using a single-shot, gradient echo-planar pulse sequence with lipid suppression, with the following parameters: number of volumes = 150, repetition time (TR) = 2000 ms, echo times (TE) = 29 ms, flip angle = 75°, field of view (FOV) = 240 mm, matrix size = 64 × 64, 33 slices, voxel size = 3.75 × 3.75 × 4.55 mm^3. High-resolution T1-weighted sMRI images were collected using a multiecho MP-RAGE sequence (five echoes) with parameters: TE = 1.64, 3.5, 5.36, 7.22, 9.08 ms, TR = 2.53 seconds, Inversion Time) = 1.2 seconds, flip angle = 7°, number of excitations = 1, slice thickness = 1 mm, FOV = 256 mm, resolution = 256 × 256. The first image from each acquisition was removed to account for T1 equilibrium effects. Detailed scanning parameters are available at the COINS website. To control for head motion, we calculated the framewise displacement,[37] computed as the sum of the absolute values of the derivatives of the translational and rotational realignment estimates at each timepoint. We used a cut-off score of 0.5 (mean ± standard error: $FD_{HC} = 0.36 \pm 0.0023$, $FD_{SZ} = 0.43 \pm 0.0026$).

https://doi.org/10.1017/S1092852926100959 Published online by Cambridge University Press

fMRI data preprocessing

fMRI data preprocessing was carried out using built-in MATLAB (MathWorks, Natick, MA, United States) functions and the SPM12 software (http://www.fil.ion.ucl.ac.uk/spm/software/spm12/). sMRI data preprocessing included intensity nonuniformity correction and image segmentation. These steps were performed using the unified segmentation algorithm implemented in SPM12,[38] with a regularization parameter of 0.0001 and a bias-field smoothing parameter of 40 mm full-width at half-maximum (FWHM). fMRI data preprocessing included motion correction, spatial alignment to sMRI, nonlinear normalization to standard space, and spatial smoothing with a 6 mm FWHM Gaussian kernel.[20,39] These steps were performed using an automated pipeline created using SPM12 (Figure 1a).

fMRI connectivity analysis

Connectivity analysis was performed using ICA, a technique that extracts maximally independent patterns of coherent fMRI activity.[21] This technique was applied separately to each dataset. The estimation of the number of independent components (ICs) was performed using the minimum description length criterion.[21] ICs were retrieved using the FastICA algorithm, with a deflation approach and hyperbolic tangent (tanh) nonlinearity.[33] For each IC, a spatial map and an associated time series were extracted (Figure 1a). The spatial map represented the intensity of the activity across the voxels of that pattern, whereas the time series reflected its course over time.[41] To display the voxels contributing most strongly to a given IC and to allow inter-subject comparison, the intensity values in each map were scaled to Z-scores. This was done by subtracting the average intensity across voxels and dividing the resulting map by the standard deviation across voxels. The ICs corresponding to 14 known RSNs, including DMN, CIN, DAN, VAN, dorsal SMN, ventral SMN, early AN, LN, lateral PFN, medial PFN, left FPN, right FPN, parafoveal VN, and peripheral VN were identified using an automated template-matching procedure, in which each considered RSN-template was derived from our previous fMRI study.[20] Each RSN was identified as the IC showing the highest spatial correlation with its corresponding template map in Montreal Neurological Institute (MNI) space. To extend the ICA analysis from the single subjects to the group, a group-level map was obtained by performing a one-sample, one-sided *t*-test, using a mass-univariate analysis on the individual RSN maps (Figure 1b). In this approach, each voxel identified as significant in the results indicates that its mean z-score across subjects was significantly greater than zero at the group level. The resulting statistical maps were corrected for multiple comparisons across voxels using the Benjamini–Hochberg false discovery rate (BH-FDR) procedure.[42] The significance threshold for each RSN group-level map was set to $q < 0.01$, BH-FDR corrected. Comparison between the SZ and HC groups was performed, separately for each RSN, by using a two-sample t-test for the individual RSN maps to detect regional differences between the two groups. The significance threshold for each RSN comparison was set to $q < 0.01$, BH-FDR corrected.

Results

The final dataset included 74 SZ patients and 74 HC, with similar age and sex distribution (Table 1). Clinical characteristics of the SZ patients, including average age of onset, illness duration, antipsychotic treatment (converted to olanzapine and chlorpromazine equivalents), and PANSS scores are also reported in Table 1. All patients were in the chronic phase of the disease and were receiving antipsychotic treatment.

We analyzed the spatial maps of 14 RSNs extracted with single-subject ICA for SZ patients and HC, followed by statistical comparison to identify voxel-wise differences between the two groups. Statistical maps showed significant differences ($q < 0.01$, BH-FDR corrected) between the two groups in each network in terms of increased or decreased connectivity patterns.

The complete list of the altered RSN connectivity patterns in SZ patients compared to HC is summarized in Table 2.

The DMN in SZ patients showed reduced connectivity in left frontal eye fields (BA 8), and increased connectivity in left and right secondary visual cortex (BA 18) and left visual association area (BA 19) (Figure 2).

The CIN in SZ patients showed reduced connectivity in left and right premotor area and supplementary motor area (SMA) (BA 6), left and right broca opercular area (BA 44), left visuomotor area (BA 7), right supramarginal gyrus (BA 40), and left subgenual area (BA 25), while increased connectivity was present in left dorsal posterior cingulate cortex (PCC) (BA 31) Figure 3.

The DAN in SZ patients showed reduced connectivity in right premotor area and SMA (BA 6) and right frontal eye fields (BA 8) and increased connectivity in right secondary visual cortex (BA 18) and left angular gyrus (BA 39) (Supplementary Figure S1), whereas the VAN in SZ patients showed reduced connectivity in right frontal eye fields (BA 8) and right inferior temporal gyrus (BA 20) (Supplementary Figure S2).

The dorsal SMN in SZ patients showed reduced connectivity in right primary somatosensory cortex (BA 1) and right Visuomotor area (BA 7) and increased connectivity in right premotor area and SMA (BA 6) and right frontal eye fields (BA 8) (Supplementary Figure S3). The ventral SMN in SZ patients showed reduced connectivity in left visual association area (BA 19), left and right superior temporal gyrus (BA 22), and right angular gyrus (BA 39) and increased connectivity in left and right premotor area and SMA (BA 6), left broca opercular area (BA 44), left inferior temporal gyrus (BA 20), and right caudate (Figure 4).

The early AN in SZ patients showed reduced connectivity in left superior temporal gyrus (BA 22), right angular gyrus (BA 39), and right supramarginal gyrus (BA 40), and the LN in SZ patients showed reduced connectivity in right insula (BA 13) and right premotor area and SMA (BA 6) (Supplementary Figures S4 and S5, respectively).

The lateral PFN in SZ patients showed increased connectivity in right ventral anterior cingulate cortex (ACC) (BA 24), left primary visual cortex (BA 17), and left anterior prefrontal cortex (PFC) (BA 10) (Supplementary Figure S6). The medial PFN in SZ patients showed reduced connectivity in left visuomotor area (BA 7), left caudate, left and right nucleus accumbens, left putamen, and left hippocampus and increased connectivity in right dorsolateral PFC (BA 46) (Figure 5).

The left FPN in SZ patients showed reduced connectivity in left fusiform gyrus (BA 37), left and right parahippocampal gyrus (BA 36), and left and right hippocampus and increased connectivity in left superior temporal gyrus (BA 22), left supramarginal gyrus (BA 40), and left primary auditory cortex (BA 41) (Figure 6).

The right FPN in SZ patients showed reduced connectivity in right pars orbitalis (BA 47) (Supplementary Figure S7).

The parafoveal VN in SZ patients showed increased connectivity left secondary visual cortex (BA 18) and left visual association area (BA 19), whereas the peripheral VN in SZ patients showed reduced connectivity in left anterior PFC (BA 10) and right caudate

https://doi.org/10.1017/S1092852926100959 Published online by Cambridge University Press

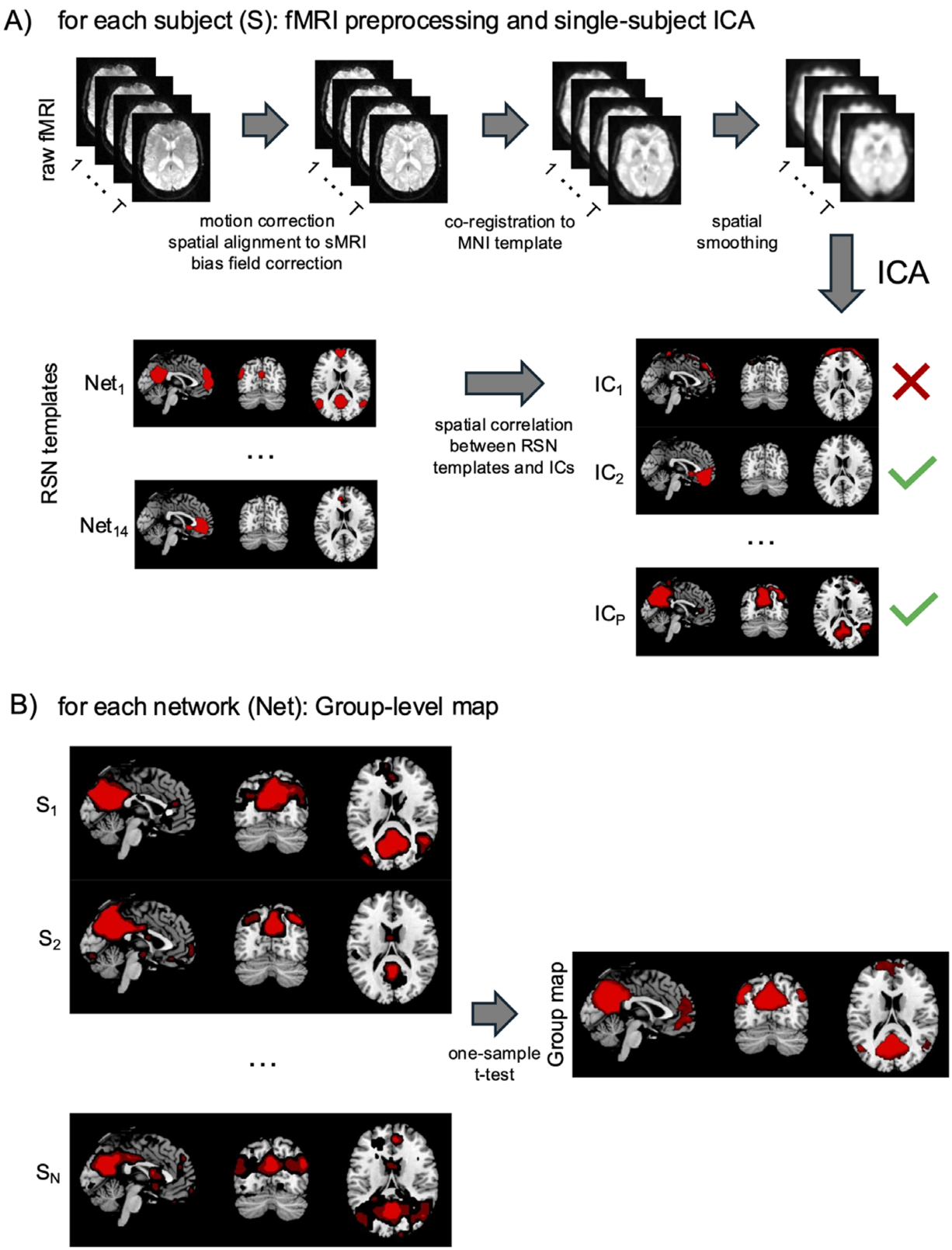


Figure 1. Automated workflow to obtain RSNs from fMRI data. This procedure is performed separately for each subject and includes the following steps: **(A)** *fMRI data preprocessing and single-subject ICA.* Raw fMRI data (with T representing the number of acquired volumes) are motion-corrected and spatially aligned to the individual sMRI. After bias field correction, the fMRI images are co-registered to the MNI template to transition from individual to standard space. The images are then spatially smoothed with a 6-mm full-width at half-maximum kernel. Independent component analysis (ICA) is performed, and the number of independent components (ICs, P) is estimated using the minimum description length criterion.[40] Some ICs represent artifacts (indicated by red crosses), while others reflect neural contributions and are associated with distinct RSNs (green checkmarks). This study considers 14 well-known RSNs. To identify neural ICs, spatial correlations between RSN templates and ICs are calculated. ICs with the highest correlation to a specific RSN template are matched, and the RSN name is assigned to the IC. For example, in this figure, $\mathbf{Net_1}$ corresponds to the default mode network (DMN) template and shows the highest correlation with $\mathbf{IC_2}$, making $\mathbf{IC_2}$ the single-subject DMN map. Similarly, $\mathbf{Net_P}$ corresponds to the medial prefrontal network (PFN) template and is matched with $\mathbf{IC_P}$, representing the single-subject PFN map for the same subject. **(B)** *Group-level correlation maps.* Group maps for each network (**Net**) are obtained by combining the single-subject RSN maps. First, single-subject RSN maps are scaled to Z-scores for inter-subject comparison. Then, a one-sample t-test is applied to generate the group-level map.

https://doi.org/10.1017/S1092852926100959 Published online by Cambridge University Press

Table 1. Demographic and clinical characteristics of the studied sample

		SZ (n = 74)	HC (n = 74)	Statistics
Age		37.43 ± 14.02	37.88 ± 12.69	$t_{146} = -0.20$, *n.s.*
Sex (M/F)		59/15	54/20	$\chi^2 = 0.93$, *n.s.*
Age of onset (years)		22.61 ± 8.85	–	–
Illness duration (years)		14.82 ± 12.33	–	–
Total olanzapine equivalent dose (mg)		14.72 ± 10.46	–	–
Total chlorpromazine equivalent dose (mg)		379.06 ± 300.78	–	–
PANSS	Positive symptoms scale	15.00 ± 4.84	–	–
	Negative symptoms scale	15.05 ± 5.52	–	–
	General psychopathology scale	28.57 ± 8.78	–	–

Note: Mean ± standard deviation of age, age of onset, illness duration, pharmacological treatment, and PANSS scores were considered.

Table 2. Summary of the fMRI RSN altered pattern in SZ patients compared to HC

	MNI	Region of altered functional connectivity in SZ patients (vs. healthy adults)
DMN	−7, 29, 60	↓Left frontal eye fields (8)
	−7, −92, 23	↑Left secondary visual cortex (18)
	6, −90, 25	↑Right secondary visual cortex (18)
	−26, −78, 25	↑Left visual association area (19)
CIN	−7, −9, 59/−52, 2, 29	↓Left premotor area and SMA (6)
	46, 4, 31	↓Right premotor area and SMA (6)
	−52, 4, 24	↓Left broca opercular area (44)
	45, 4, 25	↓Right opercular area (44)
	−7, −48, 70	↓Left visuomotor area (7)
	60, −38, 29	↓Right supramarginal gyrus (40)
	−7, 16, −17	↓Left subgenual area (25)
	−7, −62, 40	↑Left dorsal PCC (31)
DAN	28, 10, 58	↓Right premotor area and SMA (6)
	28, 9, 46	↓Right frontal eye fields (8)
	28, −51, 3	↑Right secondary visual cortex (18)
	−62, −47, 20	↑Left angular gyrus (39)
VAN	12, 23, 50	↓Right frontal eye fields (8)
	51, −1, 36	↓Right inferior temporal gyrus (20)
Dorsal SMN	36, −32, 50	↓Right primary somatosensory cortex (1)
	18, −48, 58	↓Right visuomotor area (7)
	8, 4, 65	↑Right premotor area and SMA (6)
	37, 1, 57	↑Right premotor area and SMA (6)
	8, 26, 56	↑Right frontal eye fields (8)
Ventral SMN	−50, −77, 12	↓Left visual association area (19)
	−50, 6, −10	↓Left superior temporal gyrus (22)
	54, 0, −3	↓Right superior temporal gyrus (22)
	63, −55, 17	↓Right angular gyrus (39)
	−50, 1, 20	↑Left premotor area and SMA (6)
	51, −2, 17	↑Right premotor area and SMA (6)
	−50, 3, 24	↑Left broca opercular area (44)
	−50, −19, −25	↑Left inferior temporal gyrus (20)
	17, 4, 17	↑Right caudate
Early AN	−43, −13, −8	↓Left superior temporal gyrus (22)
	52, −59, 19	↓Right angular gyrus (39)
	45, −32, 16	↓Right supramarginal gyrus (40)
LN	30, 26, −2	↓Right insula (13)
	26, 10, 59	↓Right premotor area and SMA (6)
Lateral PFN	1, −11, 33	↑Right ventral ACC (24)
	−10, −81, 5	↑Left primary visual cortex (17)
	−10, 63, 2	↑Left anterior PFC (10)
Medial PFN	−6, −58, 55	↓Left visuomotor area (7)
	−9, 6, −10	↓Left caudate
	−6, 6, −12	↓Left nucleus accumbens
	13, 7, −10	↓Right nucleus accumbens
	−15, 6, −9	↓Left putamen
	−25/−33, −25, −12	↓Left hippocampus
	49, 36, 14	↑Right (dorso)lateral PFC (46)
Left FPN	−51, −57, −16	↓Left fusiform gyrus (37)
	−25, −28, −14	↓Left parahippocampal gyrus (36)
	25, −28, 13	↓Right parahippocampal gyrus (36)
	−31, −26, −14	↓Left hippocampus
	32, −26, −13	↓Right hippocampus
	−50, −34, 18	↑Left superior temporal gyrus (22)
	−50, −31, 15	↑Left supramarginal gyrus (40)
	−50, −29, 12	↑Left primary auditory cortex (41)
Right FPN	52, 25, −8	↓Right pars orbitalis (47)
Parafoveal VN	−11, −80, 25	↑Left secondary visual cortex (18)
	−13, −80, 29	↑Left visual association area (19)
Peripheral VN	−21, 67, 9	↓Left anterior PFC (10)
	16, 11, 9	↓Right caudate
	−51, −73, 9	↑Left visual association area (19)
	−31, −62/ −53, −23	↑Left cerebellum lobule VI

Note: Blue arrows = lower functional connectivity in SZ versus HC; Red arrows = higher functional connectivity in SZ versus HC; BA, Brodmann area.

https://doi.org/10.1017/S1092852926100959 Published online by Cambridge University Press

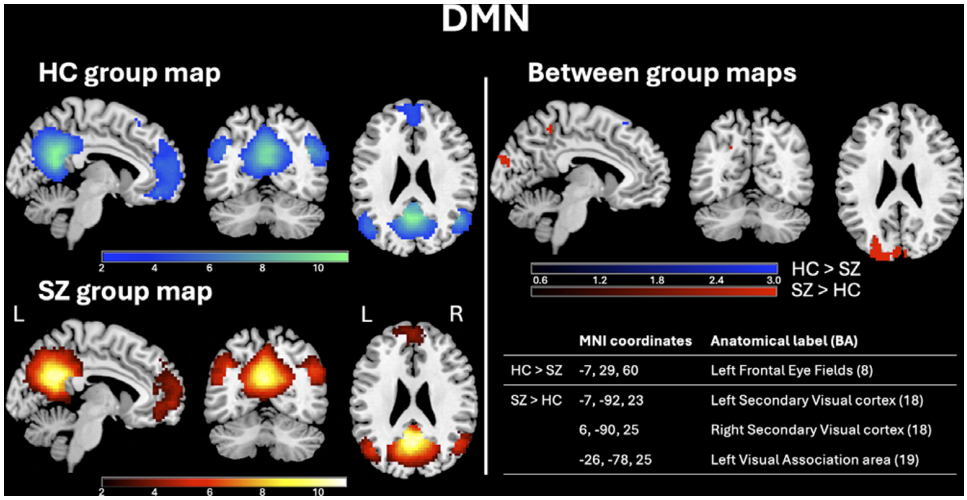


Figure 2. DMN group maps in HC and SZ patients and between-group statistical maps. Left panel: Random-effects group-level maps for the DMN in HC (top row, blue color scale) and SZ patients (bottom row, red color scale). Right panel: Random-effects group-level *t*-map for the difference between HC and SZ patients (blue/red color scales depending on the group contrast). The reported *q*-values (<0.01) were corrected for the FDR both for the random-effects group-level *t*-maps of each group and for the random-effects group-level *t*-maps of their comparison.

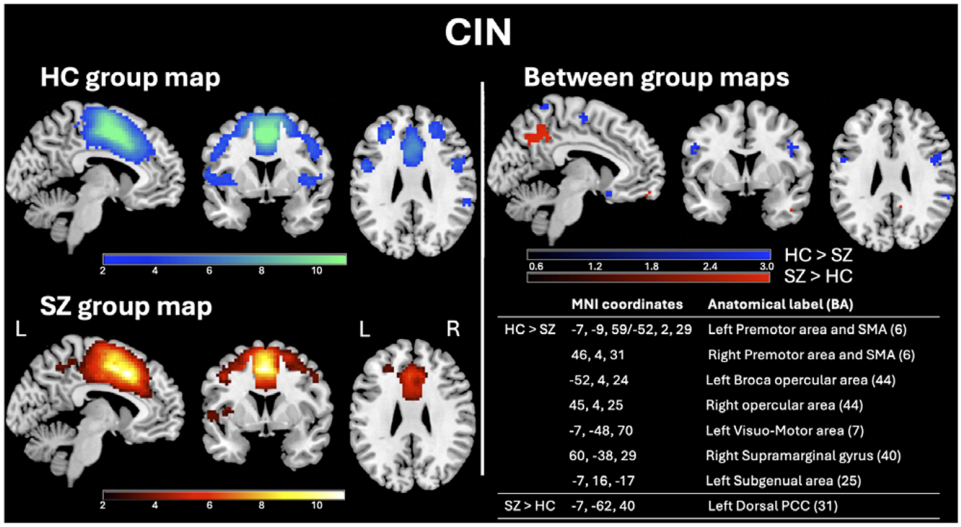


Figure 3. CIN group maps in HC and SZ patients and between-group statistical maps. Left panel: Random-effects group-level maps for the CIN in HC (top row, blue color scale) and SZ patients (bottom row, red color scale). Right panel: Random-effects group-level *t*-map for the difference between HC and SZ patients (blue/red color scales depending on the group contrast). The reported *q*-values (<0.01) were corrected for the FDR both for the random-effects group-level *t*-maps of each group and for the random-effects group-level *t*-maps of their comparison.

and increased connectivity in left visual association area (BA 19) and left cerebellum lobule VI (Supplementary Figures S8 and S9, respectively).

Discussion

RSNs are fundamental components of the brain functional architecture, as they represent patterns of spontaneous brain activity, distinctively contributing to sensory, motor, and cognitive functions. The rs-fMRI approach is particularly useful for studying individuals with limited task compliance, such as patients with SZ, a severe psychiatric illness consistently conceptualized as a dysconnectivity disorder. Indeed, SZ is characterized by disrupted functional connectivity across a range of RSNs, including the DMN and the CIN, among others.[43] These disruptions are often heterogeneous across individuals in both the magnitude and direction of connectivity alterations.

Despite advances in RSN research, a gap remains in the detailed spatial mapping of RSNs in SZ patients. To address this, in the present study, we employed single-subject ICA, a data-driven method that allows network extraction while preserving individual variability, to investigate spatial alterations in 14 distinct RSNs in SZ patients compared to HCs. By using single-subject ICA, it is possible to identify specific alterations that support a deeper understanding of the individual neurobiological underpinnings of this disorder. Such alterations could correlate with distinct symptom dimensions, such as positive or negative symptoms, cognitive deficits, or treatment response,[44] potentially revealing a more relevant relationship between connectivity patterns and clinical

https://doi.org/10.1017/S1092852926100959 Published online by Cambridge University Press

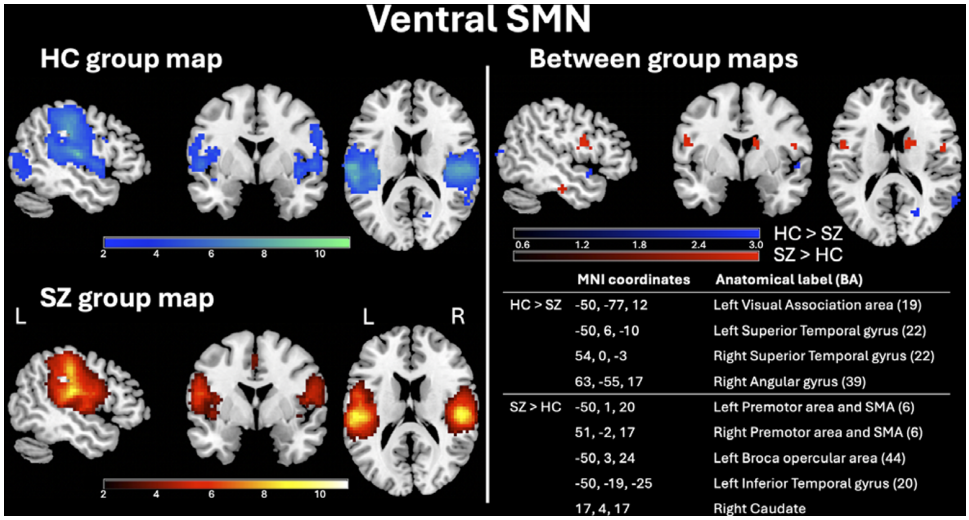


Figure 4. Ventral SMN group maps in HC and SZ patients and between-group statistical **maps.** Left panel: Random-effects group-level maps for the ventral SMN in HC (top row, blue color scale) and SZ patients (bottom row, red color scale). Right panel: Random-effects group-level *t*-map for the difference between HC and SZ patients (blue/red color scales depending on the group contrast). The reported *q*-values (<0.01) were corrected for the FDR both for the random-effects group-level *t*-maps of each group and for the random-effects group-level *t*-maps of their comparison.

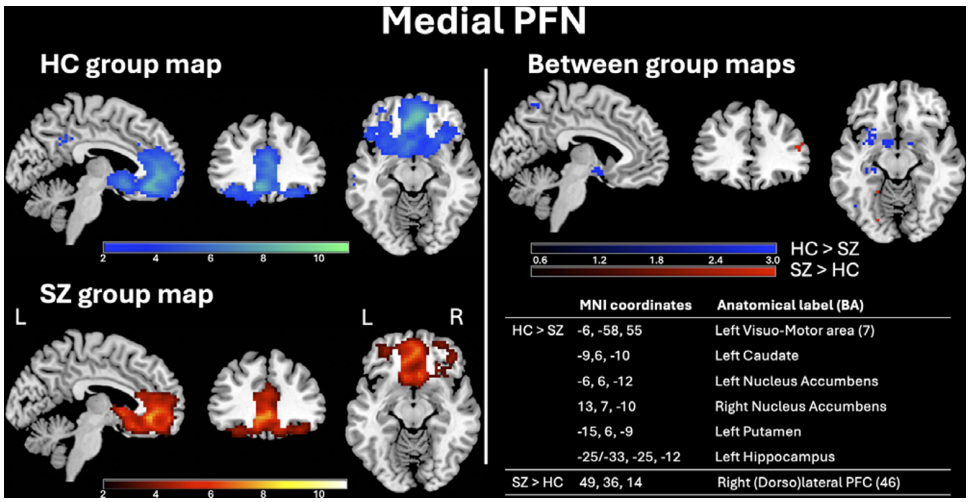


Figure 5. Medial PFN group maps in HC and SZ patients and between-group statistical **maps.** Left panel: Random-effects group-level maps for the medial PFN in HC (top row, blue color scale) and SZ patients (bottom row, red color scale). Right panel: Random-effects group-level *t*-map for the difference between HC and SZ patients (blue/red color scales depending on the group contrast). The reported *q*-values (<0.01) were corrected for the FDR both for the random-effects group-level *t*-maps of each group and for the random-effects group-level *t*-maps of their comparison.

symptoms. By uncovering unique connectivity patterns, clinicians may be better equipped to relate specific RSN dysfunctions to a patient's symptomatology and disease progression. Importantly, single-subject ICA is highly sensitive to subtle differences in brain network connectivity, and this sensitivity could be crucial for monitoring the clinical course of SZ, where symptoms may fluctuate over time, and RSN alterations might evolve in subtle or idiosyncratic ways. In this way, biomarkers that distinguish SZ from other disorders, as well as transdiagnostic markers, could be uncovered.

Our findings demonstrate widespread alterations in regions primarily involved in visual, motor, and cognitive processes, in SZ patients compared to HCs. Specifically, we observed altered connectivity patterns in several visual areas, including the primary and secondary visual cortices, frontal eye fields, visual association areas, and fusiform gyrus. These regions exhibited either lower connectivity or, in most cases, higher connectivity—not only within the two primary visual RSNs (ie the parafoveal and peripheral VSs) but also within networks where these areas are not typically considered critical or even accounted for in theory-driven approaches (eg seed-based analysis).[45] Notably, we found that visual areas were altered within the DAN, VAN, dorsal SMN, lateral PFN, lFPN, and DMN. Interestingly, all the alterations we observed within the DMN were located in visual areas. An impaired intrinsic functional connectivity in the visual system has increasingly been identified in SZ,[46,47] leading to the hypothesis that this disruption might be a potential mechanism underlying the visual abnormalities occurring in this disorder, such as blurred vision or

https://doi.org/10.1017/S1092852926100959 Published online by Cambridge University Press

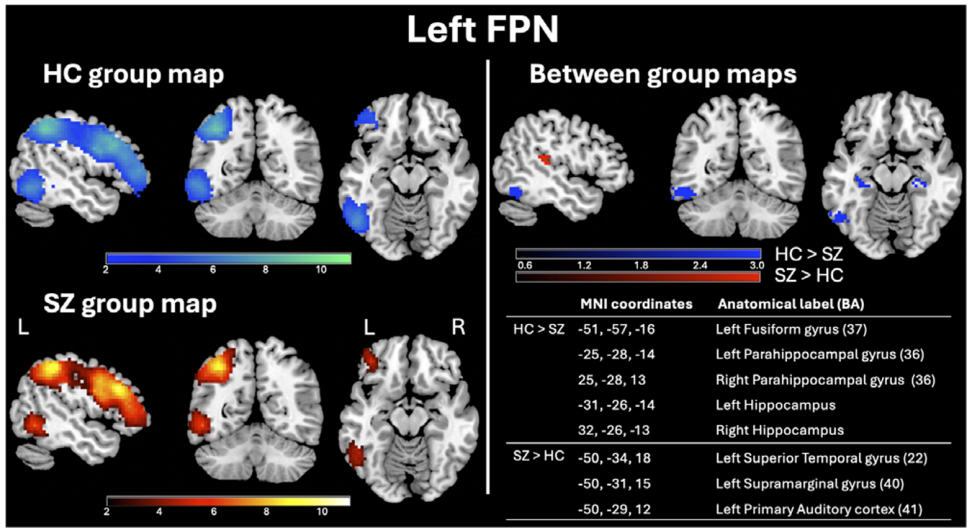


Figure 6. Left FPN group maps in HC and SZ patients and between-group statistical maps. Left panel: Random-effects group-level maps for the left FPN in HC (top row, blue color scale) and SZ patients (bottom row, red color scale). Right panel: Random-effects group-level *t*-map for the difference between HC and SZ patients (blue/red color scales depending on the group contrast). The reported *q*-values (<0.01) were corrected for the FDR both for the random-effects group-level *t*-maps of each group and for the random-effects group-level *t*-maps of their comparison.

visual hypersensitivity.[48] Alterations in visual areas have also been hypothesized to be associated with key symptoms of SZ, such as visual hallucinations and paranoia.[49,50] In line with this, it is plausible that the hyperconnectivity of visual areas observed across various networks may be linked to the visual hypermonitoring and hypervigilance characteristic of paranoia. Changes in visual areas could contribute to paranoia by disrupting how visual information is processed, interpreted, and integrated with other cognitive systems, such as attentional networks and the DMN.

Motor regions were also extensively altered in our SZ sample. Bilateral premotor areas, the SMA, and visuomotor areas exhibited connectivity alterations across the dorsal and ventral SMN, CIN, DAN, LN, and medial PFN. These results confirm the importance of using a data-driven approach like ICA for network extraction to avoid the a priori exclusion of regions not canonically included in RSNs, thus potentially missing critical insights into the disorder's pathophysiology. SZ patients frequently exhibit motor deficits, including psychomotor retardation, psychomotor agitation, and dyskinetic syndrome.[51] Previous studies have hypothesized that altered motor network connectivity might contribute to these symptoms.[52,53] Our findings suggest that alterations in motor regions extend beyond proper motor networks. For instance, the left visuomotor area, bilateral premotor areas, and SMA were all hypoconnected within the CIN, an RSN specialized in multimodal integration of cognitive and affective processing,[30] highlighting a possible interrelationship between psychopathological, cognitive, and motor symptoms in SZ.[54]

Furthermore, we found several alterations in regions associated with cognitive processes such as executive functions (eg anterior and dorsolateral PFC), language (eg Broca's opercular area and superior temporal gyrus), and reward and motivation mechanisms (eg nucleus accumbens and caudate). Additionally, lower connectivity was observed in the bilateral hippocampi and parahippocampal gyri within the left FPN, with the left hippocampus also showing hypoconnectivity within the medial PFN. This finding aligns with a substantial body of literature demonstrating hippocampal involvement in SZ pathophysiology, particularly regarding its role in memory and learning processes.[55,56] The hippocampus and parahippocampal gyri are integral to declarative memory impairments (especially episodic memory)[57] that are frequently observed in SZ.[58] Our findings suggest that altered connectivity in these regions might disrupt the coordination required for integrating memory-related information, associative learning, and higher-order cognitive control.

Considering the spatial differences between SZ patients and HC within the 14 RSNs we analyzed, the CIN, the ventral SMN, the medial PFN, and the left FPN were characterized by the most extensive alterations. Within the CIN, SZ patients showed widespread altered connectivity patterns, mostly in the form of decreased connectivity. These results are meaningful in light of the hypothesis that CIN alterations might represent common neural substrates across various psychiatric disorders, including SZ, and that these alterations might determine a disruption in the mediation processes between cognition and emotion.[30] Indeed, the component brain regions of the CIN play key roles in maintaining alertness to execute cognitive tasks,[59] sustaining intrinsic vigilance and processing high-priority information,[60] and beginning and carrying out task performances,[61] all of which are compromised in SZ patients.[62] Findings from Sasidharan et al. highlighted the central role of the CIN in the cognitive impairments observed in SZ.[63] Indeed, they found CIN lower connectivity, together with abnormal EEG and fMRI markers, in SZ patients compared to HC during the execution of a task based on error processing, brain state switching, sensory integration, and self-awareness.[63]

In our SZ sample, several regions within the SMN were also altered, particularly in the ventral subdivision, in the direction of both hypoconnectivity and hyperconnectivity. Our results are in line with recent rs-fMRI studies that found aberrant intrinsic functional connectivity of the SMN in SZ patients compared to neurotypical controls, supporting the hypothesis that disturbances in somatomotor system connectivity might be important features of the clinical profile of SZ.[64,65] Notably, as in the case of the CIN, recent findings suggested that dysconnectivity within the SMN might be a transdiagnostic signature of several pathologies: Kebets et al. (2019) found lower connectivity within the SMN in patients with SZ, attention-deficit/hyperactivity disorder, bipolar disorder, and schizoaffective disorder,[66] and Huang et al. identified hypoconnectivity within the SMN as a common marker of SZ, bipolar

https://doi.org/10.1017/S1092852926100959 Published online by Cambridge University Press

disorder, and major depression.[67] Interestingly, Huang et al. also found that the SMN dysconnectivity persisted even after clinical symptoms were effectively treated, suggesting that this pattern may serve as a stable trait marker for psychiatric disorders.[67]

The medial PFN was characterized by widespread decreased connectivity patterns in SZ patients compared to HC. According to the framework proposed by Sakurai et al., molecular- and network-level abnormalities in the PFN are key contributors to the cognitive impairments occurring in SZ.[68] In particular, it has been shown how the functional connectivity of the medial PFC is involved in various cognitive processes, including decision-making and different types of memory, like perceptual, episodic-autobiographical, and prospective-guided memory.[69] Therefore, the lower connectivity observed within the PFN may be associated with deficits in these cognitive domains. Notably, alterations in the medial PFC have been replicated in SZ with multimodal imaging techniques,[70,71] leading to the hypothesis that this region, with its connections, might be a prominent site of abnormality in SZ.[70]

We also found several connectivity alterations within the left FPN, consistent with previous studies.[47,72,73] Considering its bilateral distribution, the FPN is primarily defined as a cognitive control network, which flexibly manages task adaptation and implementation in healthy conditions.[74] On the contrary, cognitive control is compromised in many forms of psychopathology: according to Marek and Dosenbach, this impairment is attributable to the atypical development of a flexible brain network like the FPN, and this may be a common feature across many disorders, including SZ, depression, and anxiety.[75] Concerning the left FPN specifically, its functional association with language processing and verbal working memory has been highlighted,[76] and the alterations in the functional connectivity within this network may contribute to cognitive deficits in SZ, as suggested by Sharma et al.[47] Therefore, given the linguistic impairments typical of SZ (eg disorganized speech, impaired verbal fluency),[77] the altered left FPN connectivity may contribute to this kind of symptoms by affecting functions that are crucial for language performance, like working memory and cognitive control.

It is important to underline the alterations we found within the DMN, which is the most studied RSN and whose alterations are the most documented in SZ.[31] While we did not find extensive differences in the spatial maps between patients and HC, we reported that all the discrepancies in connectivity between the two groups were located in visual areas, mostly showing a pattern of hyperconnectivity. This result highlights the link between visual functions and internally oriented processes, suggesting that abnormal processing of visual input may impact patients' mental activities, such as interpersonal communication and emotional interpretation (leading to social difficulties), which are cognitive functions sustained by the DMN.[78] Notably, in our previous work, we found higher connectivity between the DMN and the VS in SZ patients compared to HC.[79] This result, together with the ones from other studies,[80,81] provides further evidence in support of the early visual dysfunction hypothesis in SZ, where abnormal processing of visual input is interpreted as a marker of the tendency to psychosis or a more severe SZ syndromic profile.[82,83]

Limitations and future perspectives

Several limitations in our study should be acknowledged. First of all, despite its advantages, single-subject ICA is not without limitations. A significant drawback of this approach is the potential to overfit to noise in individual datasets. fMRI data are inherently noisy, and ICA, by relying on statistical independence, can sometimes separate noise into components that appear meaningful.[84] Additionally, the algorithm performance can be affected by the quality of the preprocessing steps,[85] which is particularly relevant in clinical populations like SZ, where motion artifacts and other confounds might be more pronounced. Nevertheless, although ICA can be sensitive to variance differences across individuals, the template-matching step was used to retain only those components showing high spatial cross-correlation with established RSN templates, thereby reducing the likelihood that noisy or biologically irrelevant components were included in the group analysis. In addition, this bottom-up strategy allows individual topological variations to be preserved, whereas these may be attenuated in approaches that impose stronger group-level spatial constraints. At the same time, we acknowledge that this approach does not guarantee the same level of correspondence across subjects as group ICA with dual regression, which may provide stronger subject-to-subject alignment of network maps.[86]

Another limitation of our study is that clinical variables were only available for the SZ group and were therefore not included as covariates in the between-group comparison model. As a result, we cannot exclude the possibility that illness duration or antipsychotic treatment contributed to part of the observed fMRI effects. Although all our patients were in the chronic phase of the disease and were receiving pharmacological treatment—thus reducing potential confounding effects related to the inclusion of first-episode or drug-free patients—we could not rule out the influence of factors such as the duration of illness and the antipsychotic treatment on the fMRI results. Future studies should explicitly model these clinical factors to clarify the extent to which the observed fMRI effects reflect disease-related mechanisms rather than variability associated with illness progression or pharmacological treatment. Finally, although the spatial maps produced by ICA can reveal functional network disruptions, future studies should address how these disruptions translate into specific clinical symptoms or cognitive impairments. More research is needed to establish clear links between individual RSN abnormalities and distinct clinical outcomes in SZ.

Conclusions

In conclusion, our findings provide compelling evidence of widespread resting-state functional connectivity alterations in SZ, not only within cognitive and affective networks, but also extending to visual and motor systems. The involvement of visual areas across multiple RSNs, particularly the DMN, underscores the importance of considering sensory processing abnormalities as core features of SZ pathophysiology. Likewise, the alterations observed in motor and cognitive control regions across different RSNs highlight the interplay between motor, cognitive, and affective symptoms. Networks such as CIN, ventral SMN, medial PFN, and left FPN emerged as particularly disrupted, supporting the notion that some connectivity abnormalities may be transdiagnostic across psychiatric disorders. These results reinforce the value of a single-subject ICA approach in uncovering subtle differences in brain network connectivity. In a clinical context, this sensitivity could be critical for monitoring the clinical course of SZ, given the temporal variability of symptoms and the subtle, potentially idiosyncratic evolution of RSN alterations, and may also help uncover biomarkers that differentiate SZ from other disorders or reveal transdiagnostic signatures. To conclude, single-subject ICA provides a powerful tool to map specific brain connectivity patterns to individual symptoms, and offers a promising framework for understanding the neurobiological underpinnings of SZ through a more individualized and nuanced analysis of RSNs.

https://doi.org/10.1017/S1092852926100959 Published online by Cambridge University Press

Supplementary material. The supplementary material for this article can be found at http://doi.org/10.1017/S1092852926100959.

Data availability statement. The raw data supporting the conclusions of this article were downloaded from COINS (https://coins.trendscenter.org), a public, virtual database for research purposes.

Acknowledgments. None.

Author contribution. Conceptualization, D.M. and C.S.; methodology, M.M., M.B., D.M. and C.S.; software, M.M. and D.M.; validation, M.M., M.B., D.M. and C.S.; formal analysis, M.M., C.S.; investigation, M.M., M.B., D.M. and C.S.; resources, D.M. and C.S.; data curation, M.M. and M.B.; writing—original draft preparation, M.B.; writing—review and editing, M.M., D.M. and C.S.; supervision, D.M. and C.S.; project administration, D.M. and C.S. All authors have read and agreed to the published version of the manuscript.

Financial support. "C.A.T.C.H. IN. HE.AD. Comparing Auditory hallucinations Throughout the Continuum: Hearing voices from INdividuals with psychosis to HEalthy ADults. The contribute of language lateralization, anxiety and personality traits"—P2022E5H38-CUP C53D23009070001 funded by the European Union-NextGenerationEU-PNRR M4.C2.1.1. PRIN PNRR DD 1409 (14/09/2022).

Disclosures. The authors declare no conflicts of interest.

AI software use. The authors declare no use of AI software to prepare the manuscript.

References

1. Gusnard DA, Raichle ME. Searching for a baseline: functional imaging and the resting human brain. *Nat Rev Neurosci*. 2001;**2**(10):685–694.
2. van den Heuvel MP, Hulshoff Pol HE. Exploring the brain network: a review on resting-state fMRI functional connectivity. *Eur Neuropsychopharmacol*. 2010;**20**(8):519–534.
3. Schmitt A, Hasan A, Gruber O, Falkai P. Schizophrenia as a disorder of disconnectivity. *Eur Arch Psychiatry Clin Neurosci*. 2011;**261**(2):S150–S154.
4. Friston KJ, Frith CD. Schizophrenia: a disconnection syndrome? *Clin Neurosci*. 1995;**3**(2):89–97.
5. Andreasen NC, Paradiso S, O'Leary DS. Cognitive dysmetria" as an integrative theory of schizophrenia: a dysfunction in cortical-subcortical-cerebellar circuitry? *Schizophr Bull*. 1998;**24**(2):203–218.
6. Pettersson-Yeo W, Allen P, Benetti S, McGuire P, Mechelli A. Dysconnectivity in schizophrenia: where are we now? *Neurosci Biobehav Rev*. 2011;**35**(5):1110–1124.
7. Harikumar A, Solovyeva KP, Misiura M, et al. Revisiting functional dysconnectivity: a review of three model frameworks in schizophrenia. *Curr Neurol Neurosci Rep*. 2023;**23**(12):937–946.
8. Karbasforoushan H, Woodward ND. Resting-state networks in schizophrenia. *Curr Top Med Chem*. 2012;**12**(21):2404–2414.
9. Fox MD, Greicius M. Clinical applications of resting state functional connectivity. *Front Syst Neurosci*. 2010;**4**:19.
10. Biswal B, Yetkin FZ, Haughton VM, Hyde JS. Functional connectivity in the motor cortex of resting human brain using echo-planar MRI. *Magn Reson Med*. 1995;**34**(4):537–541.
11. De Luca M, Beckmann CF, De Stefano N, Matthews PM, Smith SM. fMRI resting state networks define distinct modes of long-distance interactions in the human brain. *NeuroImage*. 2006;**29**(4):1359–1367.
12. Fox MD, Raichle ME. Spontaneous fluctuations in brain activity observed with functional magnetic resonance imaging. *Nat Rev Neurosci*. 2007;**8**(9):700–711.
13. Mantini D, Perrucci MG, Del Gratta C, Romani GL, Corbetta M. Electrophysiological signatures of resting state networks in the human brain. *Proc Natl Acad Sci USA*. 2007;**104**(32):13170–13175.
14. Rosazza C, Minati L. Resting-state brain networks: literature review and clinical applications. *Neurol Sci*. 2011;**32**(5):773–785.
15. Barkhof F, Haller S, Rombouts SA. Resting-state functional MR imaging: a new window to the brain. *Radiology*. 2014;**272**(1):29–49.
16. Menon V. 20 years of the default mode network: a review and synthesis. *Neuron*. 2023;**111**(16):2469–2487.
17. Raichle ME. The brain's default mode network. *Annu Rev Neurosci*. 2015;**38**:433–447.
18. Mohan A, Roberto AJ, Mohan A, et al. The significance of the default mode network (DMN) in neurological and neuropsychiatric disorders: a review. *Yale J Biol Med*. 2016;**89**(1):49–57.
19. Doucet GE, Janiri D, Howard R, O'Brien M, Andrews-Hanna JR, Frangou S. Transdiagnostic and disease-specific abnormalities in the default-mode network hubs in psychiatric disorders: a meta-analysis of resting-state functional imaging studies. *Eur Psychiatry*. 2020;**63**(1):e57.
20. Mantini D, Corbetta M, Romani GL, Orban GA, Vanduffel W. Evolutionarily novel functional networks in the human brain? *J Neurosci*. 2013;**33**(8):3259–3275.
21. Calhoun VD, Adali T, Pearlson GD, Pekar JJ. A method for making group inferences from functional MRI data using independent component analysis. *Hum Brain Mapp*. 2001;**14**(3):140–151.
22. Vaidya CJ, Gordon EM. Phenotypic variability in resting-state functional connectivity: current status. *Brain Connect*. 2013;**3**(2):99–120.
23. Russ MO, Mack W, Grama CR, Lanfermann H, Knopf M. Enactment effect in memory: evidence concerning the function of the supramarginal gyrus. *Exp Brain Res*. 2003;**149**(4):497–504.
24. Zatorre RJ, Gandour JT. Neural specializations for speech and pitch: moving beyond the dichotomies. *Philos Trans R Soc Lond Ser B Biol Sci*. 2008;**363**(1493):1087–1104.
25. Fedorenko E, Thompson-Schill SL. Reworking the language network. *Trends Cogn Sci*. 2014;**18**(3):120–126.
26. Corbetta M, Shulman GL. Control of goal-directed and stimulus-driven attention in the brain. *Nat Rev Neurosci*. 2002;**3**(3):201–215.
27. Ptak R. The frontoparietal attention network of the human brain: action, saliency, and a priority map of the environment. *Neuroscientist*. 2012;**18**(5):502–515.
28. Beckmann CF, DeLuca M, Devlin JT, Smith SM. Investigations into resting-state connectivity using independent component analysis. *Philos Trans R Soc Lond Ser B Biol Sci*. 2005;**360**(1457):1001–1013.
29. D'Argembeau A, Collette F, Van der Linden M, et al. Self-referential reflective activity and its relationship with rest: a PET study. *NeuroImage*. 2005;**25**(2):616–624.
30. Downar J, Blumberger DM, Daskalakis ZJ. The neural crossroads of psychiatric illness: an emerging target for brain stimulation. *Trends Cogn Sci*. 2016;**20**(2):107–120.
31. Hu ML, Zong XF, Mann JJ, et al. A review of the functional and anatomical default mode network in schizophrenia. *Neurosci Bull*. 2017;**33**(1):73–84.
32. Dong D, Wang Y, Chang X, Luo C, Yao D. Dysfunction of large-scale brain networks in schizophrenia: a meta-analysis of resting-state functional connectivity. *Schizophr Bull*. 2018;**44**(1):168–181.
33. Esposito F, Scarabino T, Hyvarinen A, et al. Independent component analysis of fMRI group studies by self-organizing clustering. *NeuroImage*. 2005;**25**(1):193–205.
34. Fioravanti M, Bianchi V, Cinti ME. Cognitive deficits in schizophrenia: an updated metanalysis of the scientific evidence. *BMC Psychiatry*. 2012;**12**:64
35. Kay SR, Fiszbein A, Opler LA. The positive and negative syndrome scale (PANSS) for schizophrenia. *Schizophr Bull*. 1987;**13**(2):261–276.
36. First MB, Gibbon M. The Structured Clinical Interview for DSM-IV Axis I Disorders (SCID-I) and the Structured Clinical Interview for DSM-IV Axis II Disorders (SCID-II). In Hilsenroth MJ, Segal DL, eds. *Comprehensive handbook of psychological assessment, Vol. 2: Personality assessment*. Hoboken, New Jersey: John Wiley & Sons; 2004;134–143.

https://doi.org/10.1017/S1092852926100959 Published online by Cambridge University Press

37. Power JD, Barnes KA, Snyder AZ, Schlaggar BL, Petersen SE. Spurious but systematic correlations in functional connectivity MRI networks arise from subject motion. *NeuroImage*. 2012;**59**(3):2142–2154.
38. Calhoun VD, Adali T, Pearlson GD, Pekar JJ. Spatial and temporal independent component analysis of functional MRI data containing a pair of task-related waveforms. *Hum Brain Mapp*. 2001;**13**(1):43–53.
39. Ashburner J, Friston KJ. Unified segmentation. *NeuroImage*. 2005;**26**(3): 839–851.
40. Marino M, Arcara G, Porcaro C, Mantini D. Hemodynamic correlates of electrophysiological activity in the default mode network. *Front Neurosci*. 2019;**13**:1060.
41. Mantini D, Corbetta M, Perrucci MG, Romani GL, Del Gratta C. Large-scale brain networks account for sustained and transient activity during target detection. *NeuroImage*. 2009;**44**(1):265–274.
42. Benjamini Y, Hochberg Y. Controlling the false discovery rate: a practical and powerful approach to multiple testing. *J R Stat Soc Ser B Methodol*. 1995;**57**(1):289–300.
43. Fornito A, Zalesky A, Pantelis C, Bullmore ET. Schizophrenia, neuroimaging and connectomics. *NeuroImage*. 2012;**62**(4):2296–2314.
44. Whitfield-Gabrieli S, Ford JM. Default mode network activity and connectivity in psychopathology. *Annu Rev Clin Psychol*. 2012;**8**:49–76.
45. Lee MH, Smyser CD, Shimony JS. Resting-state fMRI: a review of methods and clinical applications. *AJNR Am J Neuroradiol*. 2013;**34**(10):1866–1872.
46. van de Ven V, Rotarska Jagiela A, Oertel-Knöchel V, Linden DEJ. Reduced intrinsic visual cortical connectivity is associated with impaired perceptual closure in schizophrenia. *Neuroimage Clin*. 2017;**15**:45–52.
47. Silverstein SM. Visual perception disturbances in schizophrenia: a unified model. *Neb Symp Motiv*. 2016;**63**:77–132.
48. van Ommen M, Invernizzi A, Renken RJ, Bruggeman R, Cornelissen FW, van Laar T. Impaired functional connectivity in patients with psychosis and visual hallucinations. *medRxiv*. 2022–2005.
49. Seymour K, Stein T, Sanders LL, Guggenmos M, Theophil I, Sterzer P. Altered contextual modulation of primary visual cortex responses in schizophrenia. *Neuropsychopharmacology*. 2013;**38**(13):2607–2612.
50. Hamdioui S, Lotfi S. Psychomotor disorders in schizophrenia: a systematic review. *Middle-East J Sci Res*. 2016;**24**(4):1078–1085.
51. Bernard JA, Goen JRM, Maldonado T. A case for motor network contributions to schizophrenia symptoms: evidence from resting-state connectivity. *Hum Brain Mapp*. 2017;**38**(9):4535–4545.
52. Walther S, Stegmayer K, Federspiel A, Bohlhalter S, Wiest R, Viher PV. Aberrant hyperconnectivity in the motor system at rest is linked to motor abnormalities in schizophrenia Spectrum disorders. *Schizophr Bull*. 2017; **43**(5):982–992.
53. Moura BM, van Rooijen G, Schirmbeck F, et al. A network of psychopathological, cognitive, and motor symptoms in schizophrenia Spectrum disorders. *Schizophr Bull*. 2021;**47**(4):915–926.
54. Lieberman JA, Girgis RR, Brucato G, et al. Hippocampal dysfunction in the pathophysiology of schizophrenia: a selective review and hypothesis for early detection and intervention. *Mol Psychiatry*. 2018;**23**(8):1764–1772.
55. Tamminga CA, Stan AD, Wagner AD. The hippocampal formation in schizophrenia. *Am J Psychiatry*. 2010;**167**(10):1178–1193.
56. Guo JY, Ragland JD, Carter CS. Memory and cognition in schizophrenia. *Mol Psychiatry*. 2019;**24**(5):633–642.
57. Rasetti R, Mattay VS, White MG, et al. Altered hippocampal-parahippocampal function during stimulus encoding: a potential indicator of genetic liability for schizophrenia. *JAMA Psychiatry*. 2014;**71**(3):236–247.
58. Picard F, Sadaghiani S, Leroy C, Courvoisier DS, Maroy R, Bottlaender M. High density of nicotinic receptors in the cingulo-insular network. *NeuroImage*. 2013;**79**:42–51.
59. Sadaghiani S, Scheeringa R, Lehongre K, Morillon B, Giraud AL, Kleinschmidt A. Intrinsic connectivity networks, alpha oscillations, and tonic alertness: a simultaneous electroencephalography/functional magnetic resonance imaging study. *J Neurosci*. 2010;**30**(30):10243–10250.
60. Dosenbach NU, Visscher KM, Palmer ED, et al. A core system for the implementation of task sets. *Neuron*. 2006;**50**(5):799–812.
61. Keefe RS, Harvey PD. Cognitive impairment in schizophrenia. In: Geyer M, Gross G, eds. *Novel Antischizophrenia Treatments. Handbook of Experimental Pharmacology*. Vol. **213** Berlin, Heidelberg: Springer; 2012:11–37.
62. Sasidharan A, Nair AK, Marigowda V, Lukose A, John JP, Kutty BM. Schizophrenia patients show aberrant brain dynamics associated with gestalt-perception and corollary discharge: reflections from ERP and fMRI findings. *bioRxiv*. 2019;837831.
63. Keyvanfard F, Schmid AK, Nasiraei-Moghaddam A. Functional connectivity alterations of within and between networks in schizophrenia: a retrospective study. *Basic Clin Neurosci*. 2023;**14**(3):397–409.
64. Więcławski W, Bielski K, Jani M, Binder M, Adamczyk P. Dysconnectivity of the cerebellum and somatomotor network correlates with the severity of alogia in chronic schizophrenia. *Psychiatry Res Neuroimaging*. 2024;**345**: 111883.
65. Kebets V, Holmes AJ, Orban C, et al. Somatosensory-motor dysconnectivity spans multiple transdiagnostic dimensions of psychopathology. *Biol Psychiatry*. 2019;**86**(10):779–791.
66. Huang CC, Luo Q, Palaniyappan L, et al. Transdiagnostic and illness-specific functional dysconnectivity across schizophrenia, bipolar disorder, and major depressive disorder. *Biol Psychiatry Cogn Neurosci Neuroimaging*. 2020;**5**(5):542–553.
67. Sakurai T, Gamo NJ, Hikida T, et al. Converging models of schizophrenia--network alterations of prefrontal cortex underlying cognitive impairments. *Prog Neurobiol*. 2015;**134**:178–201.
68. Jobson DD, Hase Y, Clarkson AN, Kalaria RN. The role of the medial prefrontal cortex in cognition, ageing and dementia. *Brain Commun*. 2021; **3**(3):fcab125.
69. Pomarol-Clotet E, Canales-Rodríguez EJ, Salvador R, et al. Medial prefrontal cortex pathology in schizophrenia as revealed by convergent findings from multimodal imaging. *Mol Psychiatry*. 2010;**15**(8):823–830.
70. Yanagi M, Hosomi F, Kawakubo Y, Tsuchiya A, Ozaki S, Shirakawa O. A decrease in spontaneous activity in medial prefrontal cortex is associated with sustained hallucinations in chronic schizophrenia: an NIRS study. *Sci Rep*. 2020;**10**(1):9569.
71. Sharma A, Kumar A, Singh S, et al. Altered resting state functional connectivity in early course schizophrenia. *Psychiatry Res Neuroimaging*. 2018; **271**:17–23.
72. Tu PC, Lee YC, Chen YS, Li CT, Su TP. Schizophrenia and the brain's control network: aberrant within- and between-network connectivity of the frontoparietal network in schizophrenia. *Schizophr Res*. 2013;**147**(2–3): 339–347.
73. Chahine G, Richter A, Wolter S, Goya-Maldonado R, Gruber O. Disruptions in the left frontoparietal network underlie resting state endophenotypic markers in schizophrenia. *Hum Brain Mapp*. 2017;**38**(4): 1741–1750.
74. Zanto TP, Gazzaley A. Fronto-parietal network: flexible hub of cognitive control. *Trends Cogn Sci*. 2013;**17**(12):602–603.
75. Marek S, Dosenbach NUF. The frontoparietal network: function, electrophysiology, and importance of individual precision mapping. *Dialogues Clin Neurosci*. 2018;**20**(2):133–140.
76. Østby Y, Tamnes CK, Fjell AM, Walhovd KB. Morphometry and connectivity of the fronto-parietal verbal working memory network in development. *Neuropsychologia*. 2011;**49**(14):3854–3862.
77. Ehlen F, Montag C, Leopold K, Heinz A. Linguistic findings in persons with schizophrenia-a review of the current literature. *Front Psychol*. 2023;**14**: 1287706.
78. Peng Y, Zhang S, Zhou Y, et al. Abnormal functional connectivity based on nodes of the default mode network in first-episode drug-naive early-onset schizophrenia. *Psychiatry Res*. 2021;**295**:113578.
79. Biondi M, Marino M, Mantini D, Spironelli C. Unveiling altered connectivity between cognitive networks and cerebellum in schizophrenia. *Schizophr Res*. 2024;**271**:47–58.
80. Sasabayashi D, Takahashi T, Takayanagi Y, et al. Resting state hyperconnectivity of the default mode network in schizophrenia and clinical high-risk state for psychosis. *Cereb Cortex*. 2023;**33**(13):8456–8464.

https://doi.org/10.1017/S1092852926100959 Published online by Cambridge University Press

81. Jafri MJ, Pearlson GD, Stevens M, Calhoun VD. A method for functional network connectivity among spatially independent resting-state components in schizophrenia. *NeuroImage*. 2008;**39**(4):1666–1681.
82. Butler PD, Javitt DC. Early-stage visual processing deficits in schizophrenia. *Curr Opin Psychiatry*. 2005;**18**(2):151–157.
83. Spironelli C, Romeo Z, Maffei A, Angrilli A. Comparison of automatic visual attention in schizophrenia, bipolar disorder, and major depression: evidence from P1 event-related component. *Psychiatry Clin Neurosci*. 2019;**73**(6):331–339.
84. Calhoun VD, Eichele T, Pearlson G. Functional brain networks in schizophrenia: a review. *Front Hum Neurosci*. 2009;**3**:17.
85. Smith SM, Jenkinson M, Woolrich MW, et al. Advances in functional and structural MR image analysis and implementation as FSL. *NeuroImage*. 2004;**23**(Suppl 1):S208–S219.
86. Nickerson LD, Smith SM, Öngür D, Beckmann CF. Using dual regression to investigate network shape and amplitude in functional connectivity analyses. *Front Neurosci*. 2017;**11**:115.

https://doi.org/10.1017/S1092852926100959 Published online by Cambridge University Press